Role of long jumps in surface diffusion

O. M. Braun[1,*] and R. Ferrando[2,†]
[1]*Institute of Physics, National Ukrainian Academy of Sciences, 03650 Kiev, Ukraine*
[2]*INFM and CFSBT/CNR, Dipartimento di Fisica, Università di Genova, via Dodecaneso 33, 16146 Genova, Italy*
(Received 11 January 2002; published 21 June 2002)

We analyze a probability of atomic jumps for more than one lattice spacing in activated surface diffusion. First, we studied a role of coupling between the x and y degrees of freedom for the diffusion in a two-dimensional substrate potential. Simulation results show that in the underdamped limit the average jump length $\langle\lambda\rangle$ scales with the damping coefficient η as $\langle\lambda\rangle\propto\eta^{-\sigma_\lambda}$ with $1/2\leqslant\sigma_\lambda\lesssim 2/3$, so that the diffusion coefficient behaves as $D\propto\eta^{-\sigma}$ with $0\leqslant\sigma\lesssim 1/3$. Second, we introduced a realistic friction coefficient for the phonon damping mechanism and developed the technique for Langevin equation with a velocity-dependent friction coefficient. The study of diffusion in this model shows that long jumps play an essential role for diffusing atoms of small masses, especially in two limiting cases, in the case of a large Debye frequency of the substrate, when the rate of phonon damping is low, and in the case of a small Debye frequency, when the one-phonon damping mechanism is ineffective.

DOI: 10.1103/PhysRevE.65.061107 PACS number(s): 05.40.−a, 05.60.−k, 66.30.−h, 68.35.Fx

I. INTRODUCTION

A variety of phenomena in physics and other fields can be modeled as Brownian motion in an external periodic potential [1–3]. One particular example, the surface diffusion of atoms or small clusters, is of great fundamental and technological interest [4]. At low temperatures, $k_BT\ll\varepsilon$, where k_B is the Boltzmann constant, T is the temperature, and ε is the height of the substrate potential, the diffusion proceeds by uncorrelated thermally activated jumps over the barrier from one minimum of the external potential to another, and the diffusion coefficient takes the Arrhenius form, $D\propto A$ with $A=\exp(-\varepsilon/k_BT)$. Then, if the jump rate is known, the diffusion coefficient can be found with the help of the lattice-gas model [5,6] for any symmetry of the lattice [7]. Usually it is assumed that the atoms can jump to nearest neighboring (NN) minima of the substrate potential only. In this case the diffusion coefficient is equal to

$$D=\frac{1}{2d}R\langle\lambda^2\rangle, \tag{1}$$

where d is the dimensionality of the system ($d=1$ or 2 for surface diffusion), R is the rate of escape from a potential well (the sum of probabilities of the jumps from a given site to all neighboring sites per one time unit), and the mean-square jump length $\langle\lambda^2\rangle$ coincides with the square of the lattice constant a^2. To find the rate of atomic jumps, one has to study the diffusional dynamics, either by the molecular dynamics (MD) method, or with the help of a more simple approach based on the Langevin equation

$$m\ddot{r}+m\eta\dot{r}+dV(r)/dr=\delta F(t), \tag{2}$$

where m is the atomic mass and $V(r)$ is the substrate potential. In the Langevin equation (2), the energy exchange between the diffusing atom and the substrate is modeled by a viscous frictional force with the coefficient η and by the random force δF which corresponds to Gaussian white noise,

$$\langle\delta F(t)\,\delta F(t')\rangle=2\eta mk_BT\delta(t-t'). \tag{3}$$

A rigorous expression for the diffusion coefficient is known only in the overdamped limit, $\eta\gg\omega_0$ [here $\omega_0=(V''/m)^{1/2}$ is the frequency of atomic vibration at the minimum of the substrate potential], when the Fokker-Planck-Kramers (FPK) equation corresponded to the Langevin equations (2) and (3), reduces to a more simple Smoluchowski equation. An analytical solution is known for the one-dimensional (1D) substrate potential [8] and for the quasi-two-dimensional case of a channel with periodically varying width [9,10]. An approximate solution was found also for a two-dimensional (2D) substrate potential [11,12]. In the overdamped limit the jump rate behaves as $R\propto\eta^{-1}$ and the jumps are allowed for one lattice spacing only, $\lambda=a$, so that $D\propto\eta^{-1}$.

A typical situation in surface diffusion corresponds to a case of intermediate or low damping. In the case of intermediate frictions, $\eta\lesssim\omega_0$, the diffusion can be adequately described by the transition state theory (TST) [13], where $\lambda=a$ and the total escape rate is given by the Kramers expression [14] $R\approx\omega_0A/\pi$ which is independent on η, so that $D\propto\eta^0$. This case was studied in a number of papers [15]. Molecular dynamics predicts that there always exist atomic jumps longer than a unit lattice spacing, $\langle\lambda\rangle>a$, but the increase in the jump length is approximately compensated by the decrease in the escape rate R because of ''recrossings,'' when the atom after its jump to a NN potential well does not stop (thermalize) there but immediately jumps back to the initial well (the well of departure), so that Eq. (1) still holds.

The present paper is devoted to an interesting case of low damping, $\eta\ll\omega_0$, when long jumps may play a dominant

*Electronic address: obraun@iop.kiev.ua
†Electronic address: ferrando@fisica.unige.it

role. The problem of long (multiple) jumps, or flights, when an underdamped Brownian atom jumps over many a potential barrier before getting trapped again, has been discussed in a number of papers [16–20]. According to the famous Kramers work [14], the escape rate at low damping is restricted by slow diffusion in energy space, $R \propto \eta$. On the other hand, the probability of atomic jumps for many lattice constants is highly increased, $\langle \lambda \rangle \sim \langle v_s \rangle \tau$, where $\langle v_s \rangle \sim (\varepsilon/m)^{1/2}$ is an average velocity of the atoms that cross the energy barrier ε and $\tau \approx \eta^{-1}$ is the flight time, so that $\langle \lambda \rangle \propto \eta^{-1}$ (for a more detailed discussion see Refs. [14,17,21]). Thus the diffusion coefficient should scale as $D \propto \eta^{-1}$ for low damping. Analytical results are known for the 1D case in the $\eta \to 0$ limit only [1]. Numerical simulations are also too time consuming in the low-damping limit.

Although experiments do demonstrate the existence of atomic jumps for several lattice constants [22], a theory of this phenomenon is still not too clear. There are two factors that may significantly reduce the jump length. First, the surface diffusion always takes place in the configuration space of two (or three) dimensions. In the 2D space the path connecting adjoining sites may not coincide with the direction of the easy crossing of the saddle point. Besides, the trajectory of a long jump which goes through several saddle points may not correspond to a straight line. These effects have to reduce the probability of long jumps [23,24], so one could expect a dependence

$$\langle \lambda \rangle \propto \eta^{-\sigma_\lambda} \tag{4}$$

with $\sigma_\lambda < 1$. Because the escape rate in a multidimensional space should still behave as $R \propto \eta$ (see Ref. [25]), we come to the dependence

$$D \propto \eta^{-\sigma} \tag{5}$$

with $\sigma = 2\sigma_\lambda - 1 < 1$. In particular, Chen *et al.* [26] had found with the help of numerical simulation for the 2D substrate potential of centered-rectangular symmetry that $\sigma = 0.5$ which gives $\sigma_\lambda = 0.75$. Then, Caratti *et al.* [27] showed that σ is not universal but depends on a geometry of the substrate potential. They considered the 2D substrate potential of square symmetry without energy barriers (the "egg-carton" potential) and found that σ may vary from 0.76 to 0.64. A similar case of pure entropy barriers, when the atom diffuses in a channel of periodically varying width but without energy barriers, was recently studied in detail [10]. The simulation showed that the dependence (5) with $\sigma < 1$ in fact corresponds to a crossover region of intermediate frictions. At very low damping the diffusion coefficient again behaves as $D \propto \eta^{-1}$ analogously to the 1D activated diffusion with energy barriers. A width of the crossover interval, however, depends on the shape of the substrate potential, so different values of σ may be obtained in this region. The case of activated jumps, when the energy barriers are large, $\varepsilon \gg k_B T$, is still unclear. In particular, the simulations [10] for the activated diffusion in the channel of varying width predicted the value $\sigma = 1/3$ which gives $\sigma_\lambda = 2/3$.

Second, long jumps may exist only in the case of low damping. Generally, there are three mechanisms of damping which may be classified according to quasiparticles excited in the substrate [28]. If the adsorbed atom has a nonzero charge, it creates plasmons in the substrate during the motion (the electromagnetic damping mechanism). When the adatom is coupled with surface atoms of the substrate by chemical bonds, so that their electronic clouds overlap, the adatom motion results in creation of electron-hole pairs in the substrate (the *e-h* damping mechanism). Both these mechanisms lead to $\eta \sim 10^{-2}\omega_0$ and approximately are independent on the atomic velocity, because a frequency associated with the atomic motion is typically much lower than the plasmon frequency or the frequency corresponded to electrons on the Fermi level, $\omega_0 \ll \omega_{\rm pl}$, $\varepsilon_F/\hbar$. Finally, there always exists the phonon damping mechanism due to excitation of phonons in the substrate. The rate of this process is proportional to the density of phonon states in the substrate. Because the frequency associated with the adatom motion ω_0 may be of the same order of magnitude as the maximum frequency of phonons in the substrate (the Debye frequency ω_m), the phonon damping coefficient $\eta_{\rm ph}$ may strongly depend on the atomic velocity. To study this effect, we have to develop a corresponding technique, because the standard approach based on Langevin or FPK equations assumes $\eta =$ const. Besides, due to the phonon mechanism, the total damping coefficient may be large enough, $\eta \sim \omega_0$, thus long jumps will be completely suppressed.

The main goal of the present work is, taking into account both factors mentioned above, to find conditions when long jumps play an essential role in surface diffusion. The paper is organized as follows. First, in Sec. II we study diffusion for different variants of the 2D substrate potential. The phonon damping mechanism is introduced in Sec. III A, and the technique for solution of stochastic equations with the velocity-dependent damping coefficient is developed in Sec. III B. Then in Sec. III C we study surface diffusion with a realistic damping. Finally, Sec. IV concludes the paper with discussion of the results.

Throughout the paper we use dimensionless system of unit. The period of the substrate potential is taken as $a = 2\pi$, the energy barrier for activated diffusion is $\varepsilon = 2$, and the mass of the substrate atoms is $m_s = 1$. The temperature is measured in energy units ($k_B = 1$). In all simulations we used $T = 1/3$ which corresponds to activated diffusion ($\varepsilon/T = 6$ so that $A \approx 2.48 \times 10^{-3}$, $R_{\rm TST} = \omega_0 A/\pi \approx 7.89 \times 10^{-4}$, and $D_{\rm TST} = \frac{1}{2} R_{\rm TST} a^2 \approx 1.56 \times 10^{-2}$) but allows us to achieve a reasonable accuracy. The diffusion coefficient is calculated from the solution of the Langevin equation (with the Verlet or Runge-Kutta method, see details in Ref. [10]) by means of the memory expansion method [29,30], which avoids the numerical evaluation of asymptotic slopes.

II. DIFFUSION IN A 2D EXTERNAL POTENTIAL

Let us begin with the study of a role of two dimensionality of the substrate potential assuming that the damping coefficient η in Eqs. (2) and (3) is constant. We consider several variants of the 2D potential. First, let the potential have a shape of a channel of periodically varying width,

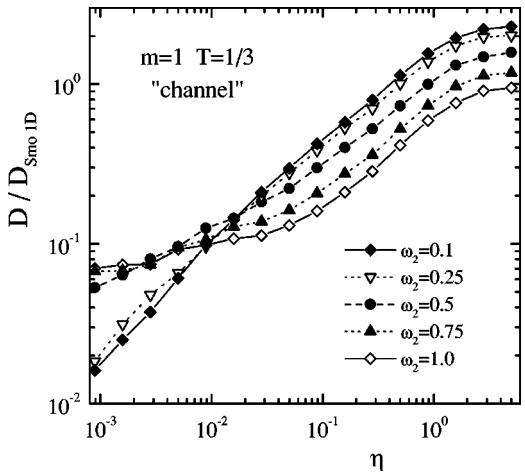

FIG. 1. Diffusion coefficient D normalized on the 1D overdamped value D_{Smo1D} as a function of the damping coefficient η for the channel of varying width, Eq. (6), for different values of the transverse curvature ω_2 at the saddle point.

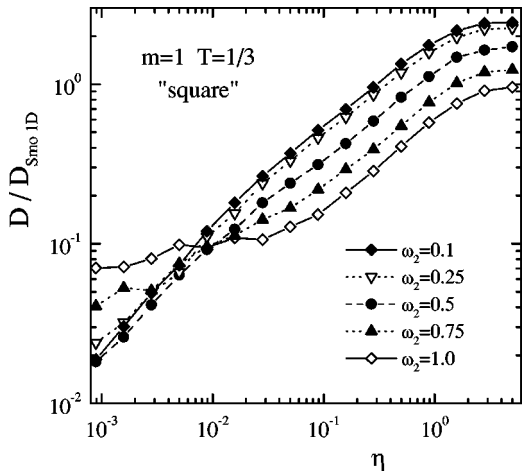

FIG. 2. The same as in Fig. 1 for the 2D substrate potential of square symmetry, Eq.(7).

$$V(x,y)=\frac{1}{2}\varepsilon(1-\cos x)+\frac{1}{2}m\omega_1^2y^2 + \frac{1}{4}m(\omega_2^2-\omega_1^2)(1-\cos x)y^2, \qquad (6)$$

where we put $\omega_1=\omega_0=1$ (through this section we assume $m=1$), so that the atomic vibrations at the minimum of the substrate potential are symmetric, and the parameter $g=\omega_1^2-\omega_2^2$ controls the coupling of the x (along the diffusion path) and y (the transverse direction) degrees of freedom. For $g=0$ the modes are decoupled, and we come to the 1D sinusoidal potential, $V_{1\mathrm{D}}(x)=1-\cos x$. At $g>0$ the saddle points are characterized by a smaller value of the transverse curvature than at the minima. The potential (6) describes a quasi-2D diffusion of atoms adsorbed on ''furrowed'' surfaces such as the (112) surface of the bcc crystal, the (110) surface of the fcc crystal, or the $(10\bar{1}0)$ surface of the hcp crystal, where the surface atoms create ''channels'' where the external atoms are adsorbed and along which they can move. Similar ''channels'' appear on the (2×1)-reconstructed (100) surface of Si.

The simulation results for the dependence of the diffusion coefficient on the damping η for a wide interval $10^{-3}\leqslant\eta\leqslant5$ and different values of the coupling between the modes are summarized in Fig. 1. The diffusion coefficient D is normalized on the exact value for the diffusion in the 1D sinusoidal potential in the overdamped limit [1], $D_{\mathrm{Smo1D}}=D_fI_0^{-2}(\varepsilon/2k_BT)$, where $D_f=k_BT/m\eta$ and I_0 is the modified Bessel function. The overdamped limit was studied analytically in Refs. [9,10]. The coupling between the modes produces the so-called entropy barriers. In the case of $g>0$, when the channel is wider at the saddle point than at the minimum, the entropy barrier is negative, so that it works against the energy barrier ε and thus leads to an increase of the diffusivity. From Fig. 1 one can see that this effect remains approximately the same for intermediate frictions down to $\eta\gtrsim0.1$. At lower damping, $\eta<0.1$, the 2D effects lead to a qualitatively different behavior. While the 1D diffusion coefficient slowly approaches the $\eta\to0$ limit $D_{\mathrm{R}}=\pi D_fA/2$ (see Ref. [1]), so that $D/D_{\mathrm{Smo1D}}\propto\eta D$ tends to a plateau, in the 2D case the value ηD continues to decrease with η. The effect becomes strong enough for the coupling $g>0.75$ ($\omega_2<0.5$).

Now let us consider a pure 2D substrate potential of square symmetry,

$$V(x,y)=\frac{1}{2}\varepsilon(1-\cos x)+m\omega_1^2(1-\cos y) + \frac{1}{2}m(\omega_2^2-\omega_1^2)(1-\cos x)(1-\cos y). \qquad (7)$$

The potential (7) describes the atoms adsorbed on the (100) surface of the bcc or fcc crystal. Along a diffusion path the potential (7) is similar to the ''channel'' potential (6), except that now both directions x and y are equivalent. The simulation results are plotted in Fig. 2. One can see that the behavior of the diffusion coefficient $D(\eta)$ is similar to that of the ''channel'' potential (6), although the 2D effects begins to play a role at smaller coupling between the modes. Already for $\omega_2=0.75$, when $g\approx0.44$, the function $D(\eta)$ essentially deviates from the 1D behavior at low damping $\eta<10^{-2}$.

The functions $D(\eta)$ for two substrate potentials (6) and (7) are compared in Figs. 3(a–c), where the error bars are also plotted. One can see that at intermediate and large frictions, $\eta>10^{-2}$, these dependences almost coincide, although the diffusivity for the square lattice is slightly higher. Moreover, at small damping ($\eta<10^{-2}$) and large enough coupling between the modes ($\omega_2<0.5$ for the ''channel'' potential and $\omega_2<0.75$ for the square potential) the functions $D(\eta)$ coincide as well within the accuracy of our simulation, and behaves according to the power law (5) with $\sigma=1/3$. In the case of square symmetry and $\omega_2=0.1$ we made simulation down to very small friction $\eta=5\times10^{-5}$ to see whether there were changes in the slope. These low-friction data also support the evidence that the slope is close to 1/3.

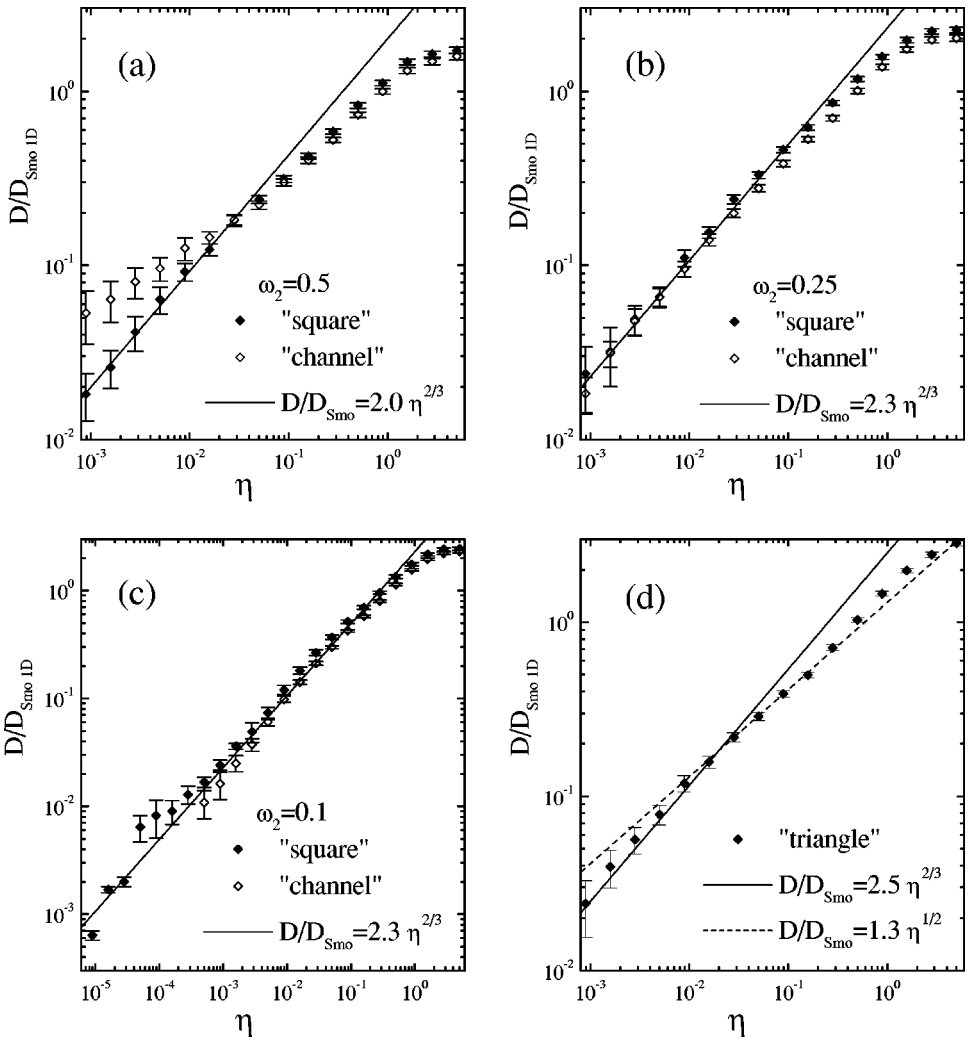

FIG. 3. The dependences $D(\eta)$ for the channel (open diamonds) and square (solid diamonds) substrate potentials for different coupling between the modes: (a) $\omega_2=0.5$, (b) $\omega_2=0.25$, (c) $\omega_2=0.1$, and (d) the same for the triangular substrate potential. The lines show the low-damping fit $D(\eta)\propto\eta^{-1/3}$. The dashed line in (d) describes the Chen *et al.* [26] fit $D(\eta)\propto\eta^{-1/2}$ for an interval of moderate damping.

As a next example we consider the ''most isotropic'' two-dimensional substrate potential, the one with the triangular symmetry,

$$V(x,y)=\frac{1}{2}\left[1-\cos x\cos\frac{y}{\sqrt{3}}+\frac{1}{2}\left(1-\cos\frac{2y}{\sqrt{3}}\right)\right]. \quad (8)$$

The minima of the potential (8) are organized into the triangular lattice with the period $a=2\pi$. The atomic vibrations at the minimum are symmetric, $\omega_x=\omega_y=\omega_0=1$. The NN minima are separated by saddle points with the barrier $\varepsilon=2$. The maxima are approximately flat and produce the hexagonal (honeycomb) lattice. The transverse frequency at the saddle point is small, $\omega_2=1/\sqrt{3}\approx 0.577$. The potential (8) is widely used in studies of atomic layers adsorbed on isotropic triangular and hexagonal substrates [31,32] as, e.g., the (111) surface of the bcc crystal. The simulation results for the triangular substrate potential are presented in Fig. 3(d). Comparing the dependence $D(\eta)$ of Fig. 3(d) with those of Figs. 3(a-c) for the potential with square symmetry, we see that again they are qualitatively similar.

In the previous work [10] we found numerically that the activated diffusion in the channel of varying width at small η can be fitted by the power law (5) with $\sigma=1/3$ both for the case of wide barriers ($g=0.99$) and the case of narrow barriers ($g=-0.99$). Figure 3 demonstrates that the same is true for pure 2D cases. Both the square potential (with different couplings $\omega_2<0.75$) and the triangular potential give the dependence $D\propto\eta^{-1/3}$. This leads to the scaling (4) of the jump length with the exponent $\sigma_\lambda=(1+\sigma)/2=2/3$. In Fig. 3(d) we plotted also the fit $D\propto\eta^{-1/2}$ proposed by Chen *et al.* [26]. One can see that such a dependence may be used for an interval of intermediate frictions only, $0.01<\eta<0.1$, but it cannot be considered as the low-damping asymptotic behavior.

To study long jumps in more detail, we calculated the distribution of jump lengths $P(\lambda)$ and the escape rate R for a fixed value of the damping coefficient $\eta=0.01$. We assumed that the atom is trapped in a given well if it has sojourned in this well for a time lapse not shorter than $(2\eta)^{-1}$ [17,19,21]. The results are presented in Figs. 4 and 5. In agreement with the results of Refs. [17,21], the distribution $P(\lambda)$ undergoes a fast drop for short jumps $\lambda=(2-3)a$ and then approaches to a slower exponential decay. Surprisingly, this drop is much larger in the 1D system than in the 2D lattice with strong coupling between the modes, the probability of jumps for several (2–5) lattice constants in the 2D system is much larger. The very long jumps ($\lambda>10a$) are, however, sup-

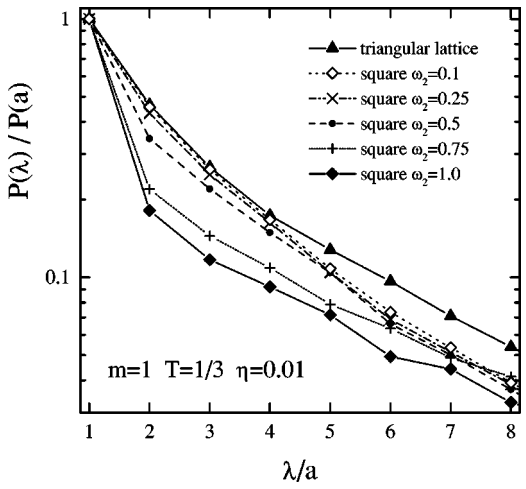

FIG. 4. Distribution of jump lengths $P(\lambda)$ for a fixed damping $\eta=0.01$ for the triangular and square substrate potentials.

pressed in the 2D system, thus the average jump length $\langle\lambda\rangle$ decreases when the coupling g becomes strong enough. According to Fig. 5, $\langle\lambda\rangle\approx 3.5a$ in the 1D case and decreases to $\langle\lambda\rangle\approx 3a$ at $\omega_2\leqslant 0.5$. The decrease in the jump length due to 2D effects is, however, not too strong. Figure 5 demonstrates also that the escape rate R grows as the coupling g increases, the escape from the 2D potential well is characterized by a higher probability.

From the simulation results presented above it becomes clear that the earlier results of Chen *et al.* [26] and Caratti *et al.* [27] correspond in fact not to the low-damping asymptotic behavior but to a crossover region of intermediate frictions. The result $\sigma=1/3$ and $\sigma_\lambda=2/3$ obtained in the present work, seems to be more close to the asymptotic values. A complete numerical study of the case of very low damping ($\eta<10^{-3}$) is, unfortunately, too time consuming. However, in the case where we calculated down to $\eta=5\times10^{-5}$ the slope obtained around $\eta=10^{-3}$ was confirmed. To find an asymptotic behavior of D and its multipliers R and

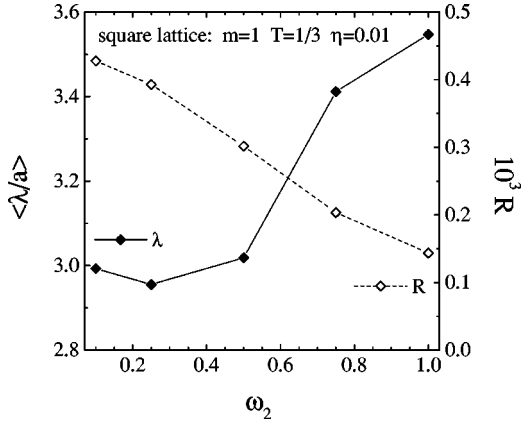

FIG. 5. Average jump length $\langle\lambda\rangle$ in units of a (left axis, solid diamonds, and solid curve) and the escape rate R (right axis, open diamond, and dashed curve) for the 2D lattice of square symmetry as functions of the transverse frequency ω_2 at the saddle point for $\eta=0.01$.

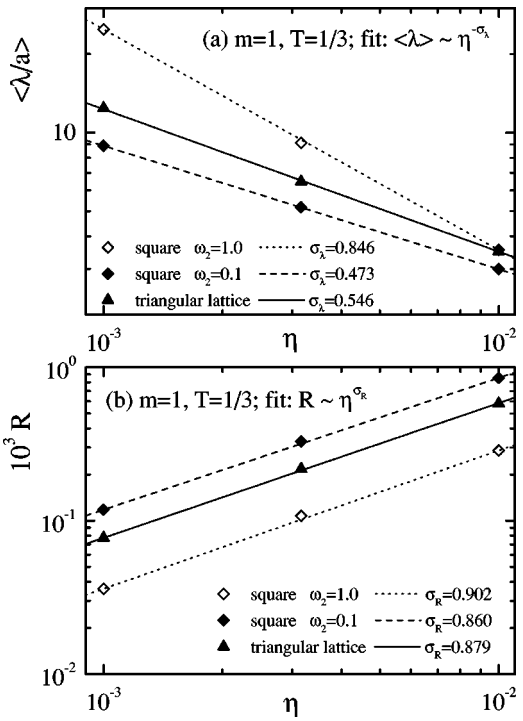

FIG. 6. (a) Average jump length $\langle\lambda\rangle$ and (b) escape rate R as functions of the damping constant η for the 1D case (open diamonds), the square potential with strong coupling $g=0.99$ (solid diamonds), and the triangular lattice (solid triangles). The lines describe the power-law fit.

$\langle\lambda\rangle$ for small η, we calculated them separately for three values of the damping in the interval $10^{-3}\leqslant\eta\leqslant10^{-2}$. The results presented in Fig. 6 can be fitted by power laws $R(\eta)\propto\eta^{\sigma_R}$ and $\langle\lambda(\eta)\rangle\propto\eta^{-\sigma_\lambda}$ with different exponents σ_R and σ_λ. The escape rate exponent $\sigma_R\approx0.9$ is close to the exact 1D value $\sigma_R=1$ which should not be changed for the 2D system [25]. A small decreasing of σ_R from 1 can be explained by a beginning of the crossover to the intermediate damping regime where $\sigma_R=0$ (e.g., see Fig. 3 in Ref. [33]). The results for the exponent σ_λ are, unfortunately, much less definite. The simulation leads to $\sigma_\lambda\sim0.45$–0.55 for the 2D system, which is much lower than the value $\sigma_\lambda=2/3\approx0.67$ predicted by the $D(\eta)\propto\eta^{-1/3}$ dependence.

Finally, we considered the case of a substrate potential of hexagonal symmetry. Contrary to the potentials discussed above, in the honeycomb lattice the path connecting the next-nearest neighboring sites does not coincide with a straight line. Thus a ballistic motion corresponded to long jumps should be suppressed, and the average jump length may be strongly reduced. We constructed the hexagonal substrate potential as a product of two triangular potentials appropriately scaled and shifted with respect to one another,

$$V(x,y)=0.64\varepsilon\left(\frac{3}{2}-\cos\frac{x}{\sqrt{3}}\cos\frac{y}{3}-\frac{1}{2}\cos\frac{2y}{3}\right)\times\left(\frac{3}{2}+\cos\frac{x}{\sqrt{3}}\cos\frac{y+\pi}{3}+\frac{1}{2}\sin\frac{4y+\pi}{6}\right). \quad (9)$$

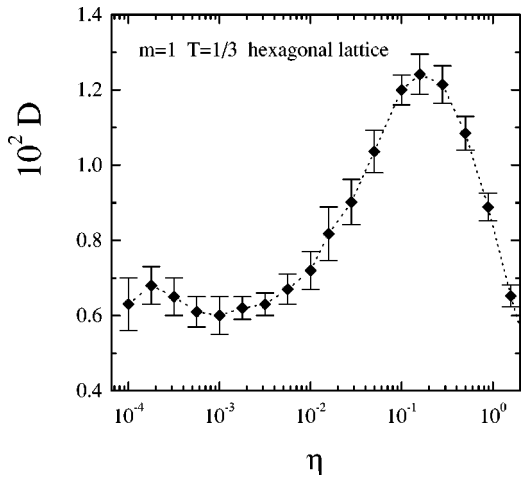

FIG. 7. Diffusion coefficient D versus the damping constant η for the substrate potential of hexagonal symmetry (9).

The minima of the potential (9) are organized in the honeycomb lattice as, e.g., on the graphite surface. The NN minima are separated by the spacing $a=2\pi$ and the energy barrier $\varepsilon=2$. The frequency of small-amplitude vibration at the bottom of the potential (9) is $\omega_0\approx 0.98$.

The simulation results for the dependence $D(\eta)$ are presented in Fig. 7. One can see that now at small frictions, $\eta<10^{-2}$, the diffusion coefficient goes to a plateau, $D\propto\eta^0$. Such a behavior reminds us that of the intermediate damping regime, when the TST operates. In the present case, however, the diffusion coefficient approximately does not depend on the friction because of the compensation of the decrease in the escape rate and the increase in the jump length as shown in Fig. 8.

Thus the simulations predict that σ_λ is within the interval $1/2\leqslant\sigma_\lambda\leqslant 2/3$. The following speculation leads to a conjecture that $\sigma_\lambda=1/2$ for all 2D systems where the x and y degrees of freedom are coupled. Indeed, if the 2D external potential $V(x,y)$ is not separable, i.e., if it cannot be presented in the form $V(x,y)=V(x)+V(y)$, the Newtonian motion in the conservative system should be stochastic in a general case [34]. For some initial conditions the atomic trajectory is regular (e.g., the atom oscillates in the same potential well or moves ballistically over the barriers), for other initial conditions the motion is chaotic and corresponds to anomalous diffusion [34,35], $\langle r^2\rangle\propto t^\nu$ with $0<\nu<1$. For the atoms that cross the barriers and have energies within a narrow "skin" layer close to $\varepsilon=2$, the atomic trajectories are close to the separatrix trajectory in the $(x,\dot{x})$ phase space, so one could expect that these trajectories will be totally chaotic and thus the motion will be pure diffusional, $\nu\approx 1$. If we now include the external damping, then in the limit $\eta\to 0$ the jumping atoms all belong to a thin skin layer of width $\sim(\eta T)^{1/2}$ (e.g., see Refs. [1,21]), so their trajectories should be close to the chaotic trajectories of the conservative system for times $t<\eta^{-1}$. Thus one could predict that $\sigma_\lambda=1/2$ and $\sigma=0$ in the $\eta\to 0$ limit.

This line of reasoning seems to work well for the case of the hexagonal honeycomb lattice, where straight trajectories are not possible, while in the other cases our data indicate that D does not saturate at $\eta\to 0$, but it increases with an exponent $\sigma\approx 1/3$.

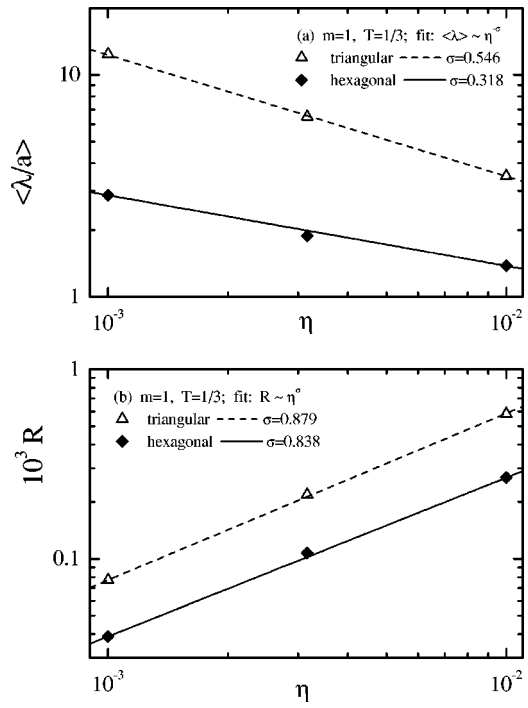

FIG. 8. (a) Average jump length $\langle\lambda\rangle$ and (b) escape rate R as functions of the damping constant η for the hexagonal potential (solid diamonds) and for the triangular lattice (open triangles). The lines describe the power-law fit.

III. DIFFUSION WITH VELOCITY-DEPENDENT DAMPING

A. Phononic damping

As was mentioned in the Introduction, the energy exchange between the moving atom and the substrate is caused by the electromagnetic and *e-h* mechanisms which are approximately independent on the atomic velocity, and by the phonon mechanism which strongly depends on the velocity. For a general atomic trajectory, the energy loss due to excitation of phonons in the substrate can be found numerically only by, e.g., the MD technique. However, for small-amplitude vibrations of the atom at the bottom of the potential well, the damping mechanisms have been studied in detail theoretically as well as experimentally by different spectroscopic methods [28]. The rate of decay of the energy of the atom vibrating with a frequency ω due to one-phonon damping mechanism is equal to [28,36]

$$\eta_{\rm ph}(\omega)=\frac{\pi}{2}\frac{m}{m_s}\omega^2\rho(\omega). \tag{10}$$

The local density of phonon state $\rho(\omega)$ at the surface of a semi-infinite crystal can in principle be calculated for any crystalline structure. However, we will use an approximate expression [36],

$$\rho(\omega)=\frac{32}{\pi}\frac{\omega^2(\omega_m^2-\omega^2)^{3/2}}{\omega_m^6}, \tag{11}$$

which has the correct behavior in the limits $\omega\to 0$ and $\omega\to\omega_m$. The one-phonon damping mechanism operates for frequencies lower than the maximum (Debye) frequency ω_m only, and its rate is small at small frequencies $\omega\ll\omega_m$, where $\eta_{\rm ph}(\omega)\propto\omega^4$. At $\omega>\omega_m$ the phonon damping is due to multiphonon mechanism and is characterized by a value [28,36] $\eta_{\rm ph}\lesssim 10^{-2}\omega_0$. The function $\eta_{\rm ph}(\omega)$, Eq. (10), achieves its maximum $\eta_{\rm ph}\approx 1.47\omega_m m/m_s$ at $\omega=(4/7)^{1/2}\omega_m\approx 0.76\omega_m$.

Although Eq. (10) describes the rate of phonon damping for the harmonic oscillations, one may expect that it will lead also to a reasonable accuracy for Brownian motion of atoms, if we will use $\omega\sim\omega_0$ for the atoms vibrating close to the bottom of the potential well, and $\omega\sim\omega_{\rm wash}\equiv(2\pi/a)\langle v\rangle$ for the atoms flying over the barriers with an average velocity $\langle v\rangle$ when the velocity oscillates with the washboard frequency $\omega_{\rm wash}$. In the Langevin equation, however, we have to use a dependence of the damping coefficient on the instant velocity of the atom [in a rigorous approach based on the $\eta(\omega)$ dependence, the diffusion will be non-Markovian and the Langevin equation has to be replaced by a more complicated integro-differential stochastic equation, see Ref. [2] and references therein]. To couple the atomic velocity with the frequency in Eq. (10), we will use the relationship $\omega=(2\pi/a)v$. Thus in what follows we use the damping coefficient

$$\eta(v)=\eta_{\rm min}+\eta_{\rm ph}(2\pi v/a), \tag{12}$$

where $\eta_{\rm min}$ describes the velocity-independent contribution to the external damping (the total action of the electromagnetic, *e-h* and multiphonon damping mechanisms), and $\eta_{\rm ph}(\omega)$ is given by Eqs. (10) and (11). In the simulation we put $\eta_{\rm min}=0.01$ which is in agreement with the discussion presented above.

The approach described above should lead to a good degree of accuracy for fast atoms that cross many saddle barriers and correspond to long jumps, which is of the main interest of the present work. As for atoms that move around well bottoms, their average velocity is $v\sim v_T=(T/m)^{1/2}$, while the vibrational frequency is $\omega_0=(\varepsilon/2m)^{1/2}$. For the parameters used in the simulations ($T=1/3$ and $\varepsilon=2$) we have $v_T\approx 0.577$ and $\omega_0=1$ for $m=1$. Thus the total damping is close to the interval of intermediate frictions, where the TST operates and the escape rate R approximately does not depend on the damping, so that the described approach should lead to a correct description of the escape rate as well.

Because the standard technique of Langevin equations assumes a constant damping coefficient, in the next subsection we develop the technique for the case when the damping depends on the velocity.

B. Langevin equation

In a general case the stochastic equation for a measurable variable $\vec{q}\equiv\{q_l\}$ has the following form [37]:

$$dq_l(t)=K_l(\vec{q})dt+\sum_m G_{lm}(\vec{q})dw_m(t),$$

$$\langle dw_m(t)\rangle=0,\quad \langle dw_l(t)dw_m(t)\rangle=\delta_{lm}dt, \tag{13}$$

where the first term in the right-hand side of the first equation of the set (13) is called the drift term and describes the action of the regular force, and the second term is called the diffusion term and describes the action of the random force. The set of equations (13) is equivalent to the Fokker-Planck equation

$$\frac{\partial f(\vec{q},t)}{\partial t}=-\sum_l\frac{\partial}{\partial q_l}[K_l(\vec{q})f(\vec{q},t)]+\frac{1}{2}\sum_{kl}\frac{\partial^2}{\partial q_k\partial q_l}\left(\sum_m G_{km}(\vec{q})G_{lm}(\vec{q})f(\vec{q},t)\right) \tag{14}$$

for the distribution function $f(\vec{q},t)$.

To obtain the Langevin equation (2), we have to put in Eq. (13) $q_1=x$ and $q_2=v$ (to shorter notations, we consider a single atom with one degree of freedom only), $K_1(x,v)=v$, $K_2(x,v)=-\eta(x,v)v-V'(x)/m$, and $G_{11}=G_{12}=G_{21}=0$. The unknown function $G_{22}(x,v)$ in Eq. (14) is coupled with the random force δF in Eq. (2) by the relationship $\delta F(x,v,t)/m=G_{22}(x,v)dw_2(t)/dt$, so that $\langle\delta F(x,v,t')\delta F(x,v,t)\rangle=m^2G_{22}^2(x,v)\delta(t-t')$. The corresponding FPK equation takes the form

$$\frac{\partial f}{\partial t}+v\frac{\partial f}{\partial x}-\frac{V'(x)}{m}\frac{\partial f}{\partial v}=\frac{\partial}{\partial v}\left[\eta(x,v)\left(v+\frac{1}{2\eta(x,v)}\frac{\partial}{\partial v}G_{22}^2(x,v)\right)f(x,v,t)\right]. \tag{15}$$

The Maxwell-Boltzmann distribution $f(x,v)\propto\exp\{-[\frac{1}{2}mv^2+V(x)]/k_BT\}$ must satisfy Eq. (15). Substituting it into Eq. (15), we obtain the following equation on the unknown function $G_{22}(x,v)$:

$$\frac{\partial G_{22}^2(x,v)}{\partial v}-\frac{mv}{k_BT}G_{22}^2(x,v)+2\eta(x,v)v=0. \tag{16}$$

It is easy to check that Eq. (16) has the solution $G_{22}^2(x,v)=2\eta_R(x,v,T)k_BT/m$, where

$$\eta_R(x,v,T)=\int_0^\infty d\epsilon e^{-\epsilon}\eta[x,\tilde{v}(\epsilon)],\tilde{v}^2(\epsilon)=v^2+\frac{2k_BT}{m}\epsilon. \tag{17}$$

Indeed, from Eq. (17) we have

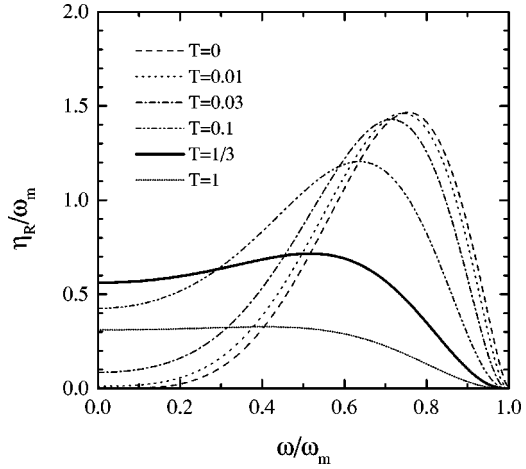

FIG. 9. The coefficient $\eta_R(\omega)$, Eq. (17), which determines the amplitude of the random force according to Eq. (21), for different temperatures.

$$\frac{k_BT}{mv}\frac{\partial\eta_R(v)}{\partial v}=\frac{k_BT}{mv}\int_0^\infty d\epsilon e^{-\epsilon}\frac{\partial\eta(\tilde{v})}{\partial\tilde{v}}\frac{v}{\tilde{v}}$$

$$=\int_{|v|}^\infty d\tilde{v}e^{-\epsilon(\tilde{v})}\frac{\partial\eta(\tilde{v})}{\partial\tilde{v}}. \qquad (18)$$

Then, integrating by parts, we obtain

$$\frac{k_BT}{mv}\frac{\partial\eta_R(v)}{\partial v}=-\eta(v)+\frac{m}{k_BT}\int_{|v|}^\infty d\tilde{v}e^{-\epsilon(\tilde{v})}\tilde{v}\,\eta(\tilde{v}), \quad (19)$$

or

$$\frac{k_BT}{mv}\frac{\partial\eta_R(v)}{\partial v}=-\eta(v)+\int_0^\infty d\epsilon e^{-\epsilon}\eta[\tilde{v}(\epsilon)]$$

$$=-\eta(v)+\eta_R(v), \qquad (20)$$

which satisfies Eq. (16).

Thus the random force $\delta F(t)$ in Eq. (2) in the case of velocity-dependent friction coefficient must be determined, instead of Eq. (3), by the correlation function

$$\langle\delta F(t)\delta F(t')\rangle=2\eta_R(v)mk_BT\delta(t-t'), \qquad (21)$$

where the coefficient $\eta_R(v)$ is defined by Eq. (17). If the external damping does not depend on the velocity, we have $\eta_R(x)=\eta(x)$, i.e., the standard expression for the random force in the Langevin equation.

The coefficient η_R as a function of the frequency $\omega=2\pi v/a$ for different temperatures T is presented in Fig. 9. One can see that a deviation of $\eta_R(\omega)$ from $\eta(\omega)$ is more essential at small frequencies and becomes important for temperatures $T>10^{-2}m\omega_m^2(a/2\pi)^2$ only.

C. Simulation results

The rate of phonon damping [Eqs. (10) and (11)] depends on the Debye frequency ω_m which is a characteristic of the substrate. To study a role of $\eta_{\rm ph}$, we made simulations for two values of ω_m, for a realistic (in our dimensionless units) value $\omega_m=10$, and also for a quite small value $\omega_m=1$ which may correspond to a soft substrate with low-frequency phonon spectrum, when the phonon damping could be very important.

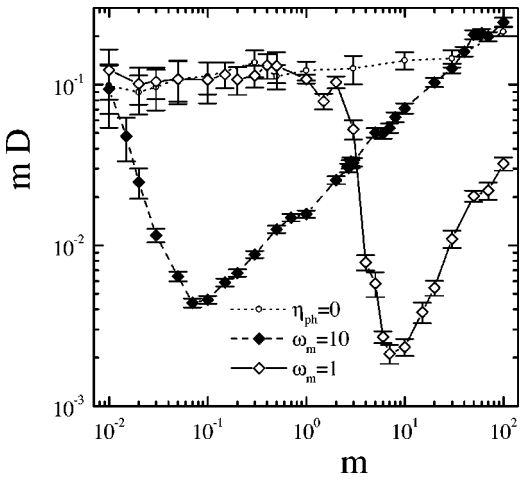

FIG. 10. Diffusion coefficient D (times the mass m) as a function of the atomic mass m for the 1D sinusoidal substrate potential with different Debye frequencies: $\omega_m=\infty$ (small open circles and dotted curve), $\omega_m=10$ (solid diamonds and dashed curve), and $\omega_m=1$ (open diamonds and solid curve).

Because we fixed the mass of the substrate atoms in our dimensionless units ($m_s=1$), now we will vary the mass of the diffusing atom in a wide range $m=10^{-2}$–10^2. In this case the frequency $\omega_0=m^{-1/2}$ changes from 10 to 0.1, so even for the largest mass $m=100$ we still have $\eta_{\rm min}\ll\omega_0$ and may occur in the regime of small or intermediate friction.

Let us first consider the one-dimensional substrate potential. The dependence of the diffusion coefficient D on the atomic mass m is presented in Fig. 10, where the functions $D(m)$ for $\omega_m=1$ and $\omega_m=10$ are compared to that for the case when the phonon damping is absent (the curve for $\omega_m=\infty$ in Fig. 10, where $\eta=\eta_{\rm min}=0.01$ so that the value of the diffusion coefficient is close to the $\eta\to0$ limiting value $D_{\rm R}=\pi D_f A/2\approx0.13/m$). Also, in Fig. 11 we show the average jump length and the escape rate as functions of m for the same values of ω_m.

Due to phonon damping the total friction coefficient increases. This leads to an increase of the escape rate R, but the average jump length $\langle\lambda\rangle$ decreases, and the common action of both effects results in a decrease of the diffusion coefficient D. Let us first consider a realistic case of $\omega_m=10$ plotted by open diamonds in Figs. 10 and 11. When the atom goes over the barrier, its energy is $\frac{1}{2}mv^2\sim\varepsilon=2$, so that $v\sim2/\sqrt{m}$. Thus, for the lowest mass $m=10^{-2}$ plotted in the figures, a characteristic atomic frequency $\omega\sim20$ is higher than the Debye frequency $\omega_m=10$, the one-phonon damping does not operate, the average jump length is large, $\langle\lambda\rangle>10\,a$, and the diffusivity is high. Then, when the mass increases within the interval $10^{-2}<m<10^{-1}$, we have $v\sim20$–6, so that the washboard frequency $\omega=2\pi v/a$ penetrates into the phonon zone, the one-phonon mechanism

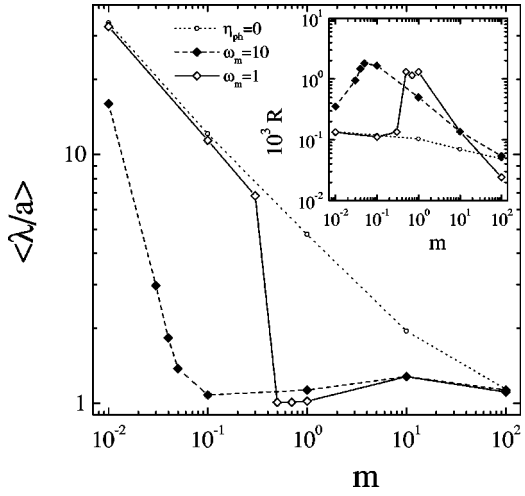

FIG. 11. Average jump length $\langle\lambda\rangle$ and the escape rate R (inset) as functions of the atomic mass m for the 1D potential with $\omega_m=\infty$ (small open circles and dotted curve), $\omega_m=10$ (solid diamonds and dashed curve), and $\omega_m=1$ (open diamonds and solid curve).

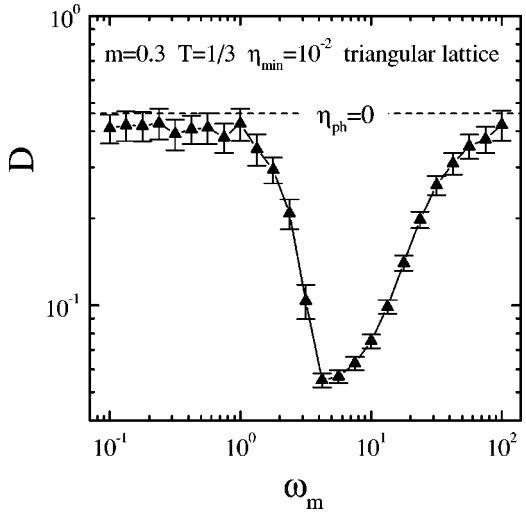

FIG. 12. Diffusion coefficient D as a function of the Debye frequency ω_m for the substrate potential of triangular symmetry ($m=0.3$, $T=1/3$, and $\eta_{\min}=0.01$).

starts to work, the damping sharply increases, goes through the largest value $\eta\sim 1.47 m\omega_m\sim 1$ corresponding to the overdamped case, and then decreases down to values corresponding to an intermediate-friction regime. Simultaneously the jump length decreases to $\langle\lambda\rangle\sim a$, while the escape rate grows as shown in Fig. 11. Then, with further increase of the mass in the interval $10^{-1}<m<10^2$, the total damping corresponds to the intermediate-friction regime, so that the jump length remains small, $\langle\lambda\rangle\gtrsim a$, and the escape rate and the diffusion coefficient decrease with m, $D\propto R\propto\omega_0\propto m^{-1/2}$. Note that for large masses, $m>10$, the phonon damping coefficient decreases back to the region of small frictions because of $\eta_{\rm ph}\propto v^4\propto m^{-2}$, but the long jumps are still suppressed due to large mass of the atom.

A similar behavior demonstrates the ''soft'' substrate with $\omega_m=1$ (see open diamonds in Figs. 10 and 11). Now the one-phonon damping mechanism comes into play at $m\approx\omega_m^{-1}=1$. It is interesting that around this point, $0.3<m<3$, the diffusion coefficient remains as high as it was for the $\eta_{\rm ph}=0$ case. Although the jump length decreases to $\langle\lambda\rangle\sim a$, the escape rate sharply grows and compensates the decrease of $\langle\lambda\rangle$.

Thus long jumps have to exist for a small mass of the diffusing atom, $m<\omega_m^{-1}$, when the atom goes over the barriers so fast that the washboard frequency exceeds the maximum phonon frequency of the substrate, $v>\omega_m a/2\pi$, and the one-phonon damping does not operate.

Finally, let us study a common action of the phonon damping and the two dimensionality of the substrate potential. We choose the substrate potential with the triangular symmetry, a relatively small mass of the diffusing atom $m=0.3$ so that long jumps may be expected, and will vary the Debye frequency in a wide range $10^{-1}\leqslant\omega_m\leqslant 10^2$. The simulation results are presented in Figs. 12–14. As expected, the diffusivity is large and the long jumps exist in two regimes, for large values of ω_m when the phonon damping coefficient is small, and for small values of ω_m when the one-phonon damping does not operate because of large velocities of atoms which cross the barriers. For intermediate values of the Debye frequency, $\omega_m\sim 3$–10, the jumps are mainly for one lattice constant. Although the escape rate is high for these Debye frequencies, in total the diffusivity is lower than in the case of absence of phonon damping. However, even in the worst case the probability of jumps longer than one lattice constant is still not negligible, $P(2a)/P(a)>0.1$, if the atomic mass is small, $m<1$.

IV. CONCLUSION

Thus in the present work we studied the role of long atomic jumps, or flights, in the activated surface diffusion. First, we analyzed the effects of two dimensionality of the substrate potential, when the x and y degrees of freedom are coupled. Simulation results predict that in the underdamped limit the average jump length scales with the damping coefficient as $\langle\lambda\rangle\propto\eta^{-\sigma_\lambda}$ with $1/2\leqslant\sigma_\lambda\leqslant 2/3$, so that the diffusion

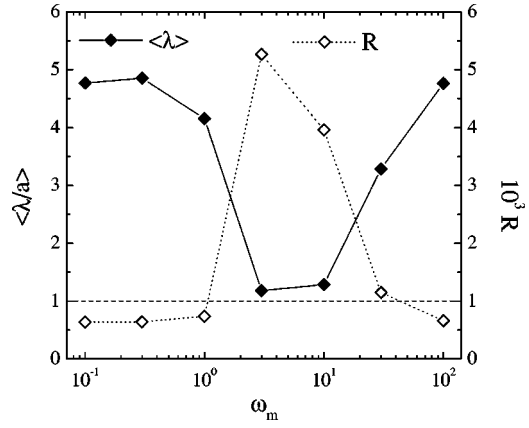

FIG. 13. Average jump length (left axes, solid diamonds) and the escape rate (right axes, open diamonds) as functions of ω_m for the triangular substrate potential.

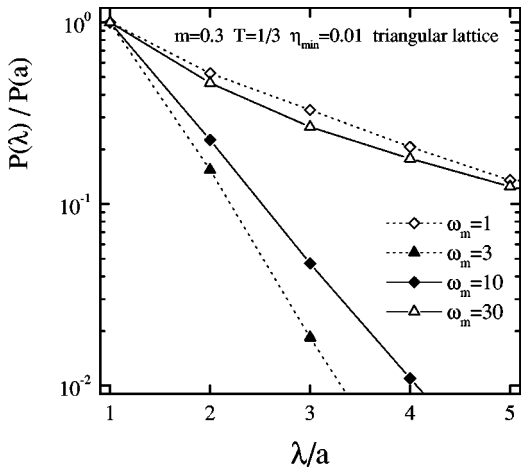

FIG. 14. Distribution of lengths of atomic jumps on the triangular lattice for a realistic velocity-dependent friction coefficient, Eq. (12), for different values of the Debye frequency.

coefficient behaves as $D \propto \eta^{-\sigma}$ with $0 \leqslant \sigma \lesssim 1/3$. One can make the conjecture that the dependence $D \propto \eta^0$ could be universal in the $\eta \to 0$ limit for all nonseparable 2D substrate potentials. Our data support this conjecture only for the hexagonal symmetry potential, which has no straight diffusion paths, while for the other potentials, which have straight diffusion paths, the exponent σ is close to 1/3.

Second, we proposed a realistic friction coefficient for the phonon damping mechanism, which describes the energy exchange between the diffusing atom and the substrate. Because the rate of phonon damping strongly depends on the frequency associated with the atomic motion, we had to develop the technique for Langevin equations with a velocity-dependent friction coefficient. The simulation of diffusion in this model showed that long jumps do exist in the case of adatoms of small masses, $m < m_s$. The long jumps are the most important in two limiting cases, in the case of a large Debye frequency of the substrate, when the rate of phonon damping is low, and in the case of a small Debye frequency, when the one-phonon damping mechanism is ineffective, because the atoms cross the barriers with a high velocity. However, in all cases the role of long jumps is not negligible. For example, for $m = 0.3 m_s$ the number of jumps for two lattice spacing substitutes more than 10% of the jumps to the NN sites.

Thus, atomic jumps over a distance of 2–3 lattice spacing are not negligible for most adsystems. The two-dimensionality effects even increase the probability of such jumps, although in total the average jump length decreases, the very long jumps are suppressed in 2D systems. The phononic damping which always operates in the case of surface diffusion, also does not kill long jumps if $m < m_s$. Thus the approach based on the lattice-gas models of surface diffusion [38], where the jumps to the NN sites are taken into account, can often claim to qualitative description only. Although it is easy to include multiple jumps in the LG model [39], the increase of the number of poorly defined parameters makes such an approach not manageable.

Experimentally long jumps can be detected using surface imaging techniques, when one makes ''snapshots'' of atomic configurations before and after an atomic jump. There are two techniques of this type, the field ion microscopy (FIM) and the scanning tunneling microscopy (STM). The FIM method, unfortunately, operates only for adatoms which do not evaporate at huge electric fields ($>10^8$ V/cm). The STM technique can in principle be used for any substrate/adatom pair, but a speed of taking a snapshot is much slower than in the FIM. For both experimental techniques one should try to follow for the motion of a single adatom and to avoid collective effects due to interaction between adatoms. The most important is to choose the adatoms which cannot penetrate into the substrate, because otherwise one may observe ''fictitious'' jumps over large distances as, e.g., in the solitonic-exchange diffusion mechanism [40]. Probably, namely such an effect was recently observed experimentally [41].

Finally, we would like to mention an interesting case of diffusion of adsorbed clusters, for example, the practically important situation of motion of Si_2 dimers on the Si(100) surface. In this case the energy exchange between the vibrational, rotational and translational degrees of freedom may strongly affect the dimer diffusivity.

ACKNOWLEDGMENT

This work was partially supported by the INTAS, Grant No. 97-31061.

[1] H. Risken, *The Fokker-Planck Equation* (Springer, Berlin, 1996).
[2] P. Hänggi, P. Talkner, and M. Borkovec, Rev. Mod. Phys. **62**, 251 (1990).
[3] V.I. Mel'nikov, Phys. Rep. **209**, 1 (1991).
[4] A.G. Naumovets and Yu.S. Vedula, Surf. Sci. Rep. **4**, 365 (1985); R. Gomer, Rep. Prog. Phys. **53**, 917 (1990).
[5] W. Dieterich, P. Fulde, and I. Peschel, Adv. Phys. **29**, 527 (1980).
[6] J.W. Haus and K.W. Kehr, Phys. Rep. **150**, 263 (1987).
[7] O.M. Braun and C.A. Sholl, Phys. Rev. B **58**, 14 870 (1998).
[8] R. L. Stratonovich, *Topics in the Theory of Random Noise* (Gordon and Breach, New York, 1967); Yu.M. Ivanchenko and L.A. Zil'berman, JETP Lett. **8**, 113 (1968); Sov. Phys. JETP **28**, 1272 (1969); V. Ambegaokar and B.I. Halperin, Phys. Rev. Lett. **22**, 1364 (1969).
[9] R. Zwanzig, Physica A **117**, 277 (1983).
[10] O.M. Braun, Phys. Rev. E **63**, 011102 (2001).
[11] T. Ala-Nissila and S.C. Ying, Phys. Rev. Lett. **65**, 879 (1990); Prog. Surf. Sci. **39**, 227 (1992).
[12] G. Caratti, R. Ferrando, R. Spadacini, and G.E. Tommei, Phys. Rev. E **54**, 4708 (1996).
[13] S. Glasstone, K. J. Laidler, and H. Eyring, *The Theory of Rate Processes* (McGraw-Hill, New York, 1941).

[14] H.A. Kramers, Physica (Amsterdam) **7**, 284 (1940).
[15] J.C. Tully, G.H. Gilmer, and J. Shugard, J. Chem. Phys. **71**, 1630 (1979); J.D. Doll and H.K. McDowell, *ibid.* **77**, 479 (1982); G. De Lorenzi and G. Jacucci, Surf. Sci. **164**, 526 (1985).
[16] E. Pollak, J. Bader, B.J. Berne, and P. Talkner, Phys. Rev. Lett. **70**, 3299 (1993).
[17] R. Ferrando, R. Spadacini, and G.E. Tommei, Phys. Rev. E **48**, 2437 (1993); **51**, 126 (1995).
[18] P. Jung and B. J. Berne, in *New Trends in Kramers' Theory*, edited by P. Talkner and P. Hänggi (Kluwer, Dordrecht, 1995), p. 67.
[19] M. Borromeo, G. Costantini, and F. Marchesoni, Phys. Rev. Lett. **82**, 2820 (1999).
[20] L.Y. Chen and S.C. Ying, Phys. Rev. B **60**, 16 965 (1999).
[21] M. Borromeo and F. Marchesoni, Phys. Rev. Lett. **84**, 203 (2000).
[22] J.W.M. Frenken, B.J. Hinch, J.P. Toennies, and Ch. Wöll, Phys. Rev. B **41**, 938 (1990); G. Ehrlich, Surf. Sci. **246**, 1 (1991); E. Ganz, S.K. Theiss, I.S. Hwang, and J. Golovchenko, Phys. Rev. Lett. **68**, 1567 (1992); J. Ellis and J.P. Toennies, *ibid.* **70**, 2118 (1993); D.C. Senft and G. Ehrlich, *ibid.* **74**, 294 (1995).
[23] V.P. Zhdanov, Surf. Sci. **214**, 289 (1989).
[24] K. Haug, G. Wahnström, and H. Metiu, J. Chem. Phys. **90**, 540 (1989); **92**, 2083 (1990).
[25] M. Borkovec and B.J. Berne, J. Chem. Phys. **82**, 794 (1985); **84**, 4327 (1986); **86**, 2444 (1987); J.E. Straub, M. Borkovec, and B.J. Berne, *ibid.* **86**, 4296 (1987).
[26] L.Y. Chen, M.R. Baldan, and S.C. Ying, Phys. Rev. B **54**, 8856 (1996).
[27] G. Caratti, R. Ferrando, R. Spadacini, and G.E. Tommei, Phys. Rev. E **55**, 4810 (1997).
[28] O.M. Braun, A.I. Volokitin, and V.P. Zhdanov, Usp. Fiz. Nauk **158**, 421 (1989) [Sov. Phys. Usp. **32**, 605 (1989)].
[29] S.C. Ying, I. Vattulainen, J. Merikoski, T. Hjelt, and T. Ala-Nissila, Phys. Rev. B **58**, 2170 (1998).
[30] T. Ala-Nissila, R. Ferrando, and S. C. Ying, Adv. Phys. **51**, 949 (2002).
[31] I. F. Lyuksyutov, A. G. Naumovets, and V. L. Pokrovsky, *Two-Dimensional Crystals* (Naukova Dumka, Kiev, 1983).
[32] R.G. Caflisch, A.N. Berker, and M. Kardar, Phys. Rev. B **31**, 4527 (1985); K. Kern and G. Comsa, in *Kinetics of Ordering and Growth at Surfaces*, edited by M. G. Lagally (Plenum Press, New York, 1990).
[33] R. Ferrando, R. Spadacini, and G.E. Tommei, Phys. Rev. A **46**, R699 (1992).
[34] A. J. Lichtenberg and M. A. Lieberman, *Regular and Stochastic Motion* (Springer-Verlag, New York, 1983).
[35] T. Geisel, A. Zacherl, and G. Radons, Phys. Rev. Lett. **59**, 2503 (1987); Z. Phys. B: Condens. Matter **71**, 117 (1988); J. Klafter and G. Zumofen, Phys. Rev. E **49**, 4873 (1994).
[36] O.M. Braun, Surf. Sci. **213**, 336 (1989); O.M. Braun and A.I. Volokitin, Fiz. Tverd. Tela **28**, 1008 (1986) [Sov. Phys. Solid State **28**, 564 (1986)].
[37] C. W. Gardiner, *Handbook of Stochastic Methods* (Springer-Verlag, Berlin, 1983).
[38] A. Danani, R. Ferrando, E. Scalas, and M. Torri, Int. J. Mod. Phys. B **11**, 2217 (1997).
[39] M. Torri and R. Ferrando, Chem. Phys. Lett. **274**, 323 (1997).
[40] O.M. Braun, T. Dauxois, and M. Peyrard, Phys. Rev. B **54**, 313 (1996).
[41] R. van Gastel, E. Somfai, W. van Saarloos, and J.W.M. Frenken, Nature (London) **408**, 665 (2000).